

Synthetic Sulfide Minerals (V)

Asahiko SUGAKI*, Hiromi SHIMA* and Arashi KITAKAZE*

1. Introduction

In order to make clear the stability of sulfide minerals, the experiments on the phase equilibrium relation of several sulfide systems have been carried out by present authors. During the experiment on the pseudo-binary system of PbS-Sb₂S₃^{1,2,3)}, synthetic minerals such as zinckenite, robinsonite and boulangerite and new synthetic phase with chemical composition of Pb₂Sb₂S₅, were synthesized. The synthesis of these minerals and Pb₂Sb₂S₅ were performed by a reaction between lead and antimony sulfides which had been prepared in advance from lead, antimony and sulfur. Lead and antimony metals used primary starting materials for the synthesis of sulfosalts are both 99.9%+ in purity. Sulfur used in purity of 99.9% as a guaranteed reagent.

On the synthetic minerals and Pb₂Sb₂S₅, their synthetic method, optical properties, X-ray powder and crystal data, and DTA cruves etc. will be described as below in this paper. The synthetic method of sevral sulfides and sulfosalts has been allready reported in detail in the previous papers^{4,5,6,7)} and then, in this paper, the method of synthesis is described briefly.

2. Pb₉Sb₂₂S₄₂ (zinckenite)

Zinckenite was known for a long time as lead-antimony sulfosalts mineral and was already produced artificialy by Iitsuka (1920)⁸⁾, Robinson (1948)^{9,10)}, Kitakaze (1968)^{1,2,3)}, Jambor (1968)¹¹⁾, Salanci and Moh (1970)¹²⁾ and others¹³⁾. It was synthesized by a solid reaction between lead sulfide (PbS) and antimony sulfide (Sb₂S₃). Antimony sulfide was prepared from a reaction between antimony and sulfur with the same method described in the previous paper⁴⁾. Lead sulfide was synthesized by reaction between lead which has platy shaped thin film obtained by cutting of ingot and granular sulfur by heating at 550°C for 6 days.

Lead and antimony sulfide were acculatly weighed with molecular ratio of nine to eleven, and were mixed thoroughly under acetone in an agate moter. Then the mixture sealed in the Hario glass tube, 8 mm in inside diameter, under vacuum in 10⁻³mm Hg by rotary vacuum pump. The sealed glass tube was heated in the electric furnace at 530°C for 5 or 6 days. Generally almost

* Department of Mining and Mineral Engineering

homogeneous lead antimony sulfosalt was obtained by first heating. After first heating, product was taken out and ground in agate moter to mix uniformly under acetone. It was again sealed in the evacuated glass tube and heated at 530°C for 6 days. It was cooled slowly in air after heating.

The synthetic product is fully sintered aggregate of acicular crystals with 0.1 to 1 mm in size and megascopically lead gray in color with metallic luster. These needle like crystals of zinckenite were shown in Fig. 1.

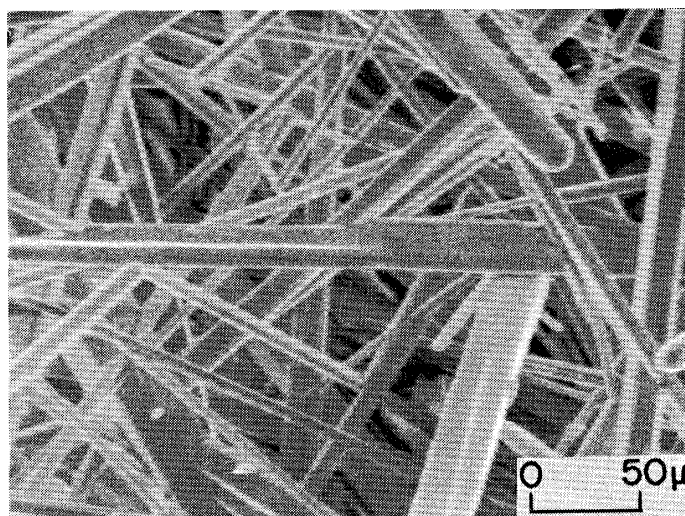


Fig. 1. Scanning electron micrograph of acicular crystals of compound $Pb_9Sb_{22}S_{42}$ synthesized at 530°C.

Under the ore microscope, synthetic zinckenit has a weak pleocroism changing its color from white to grayish white in air, and also shows strong anisotropism changing its interference color from greenish yellow to dark bluish gray under crossed nicols. Its reflection color is very similar to synthetic robinsonite.

When etched by $HNO_3(1:1)$, it quickly changes its color to brown or black. By fume of $HCl(1:1)$, it is tarnished to brown. By $KOH(sat.)$ and $HgCl_2(20\%)$, it is slightly stained to brown or bluish gray. However, it is negative for $KCN(20\%)$ and $FeCl_3(20\%)$. The optical and etching data for synthetic zinckenite were similar to those of natural zinckenite described by Short¹⁴⁾, Ramdohr¹⁵⁾ and Uytendogaadt¹⁶⁾.

The data of X-ray powder diffraction for synthetic zinckenite are given in table 1, compared that of with natural zinckenite. The cell constant was calculated from the powder data and was obtained $a=22.10\text{\AA}$, $c=4.326\text{\AA}$ which was in good accordance to Sadanaga and Takeda's value¹⁷⁾ of $a=22.10\text{\AA}$, $c=4.33\text{\AA}$. The density of sintered mass of zinckenite measured by Berman density balance was 5.36 g/cm^3 , and calculated density from the cell constant was 5.35 g/cm^3 as $Z=1$. Both of the values were in good agreement.

Table 1. The X-ray powder diffraction data for synthetic $Pb_9Sb_{22}S_{42}$

(1)		(2)			
I	d(meas.)	I	d(meas.)	(hkl)	d(calc.)
		4	11.07	(110)	11.05
1/2	5.50	16	5.530	(220)	5.525
		7	5.310	(130) (310)	5.308
1/2	4.80	3	4.790	(040) (400)	4.785
1/2	4.42	7	4.386	(320)	4.391
1	3.95	16	3.940	(021) (201)	3.942
		7	3.815	(050) (500)	3.828
		8	3.712	(211)	3.713
1	3.56	15	3.580	(031) (301)	3.580
10	3.45	100	3.441	(510) (150)	3.437
		5	3.411	(221)	3.406
1	3.36	20	3.352	(311)	3.353
		4	3.206	(041) (401)	3.209
		3	3.181	(060) (600)	3.190
		14	3.144	(340) (430)	3.146
1	3.08	13	3.080	(231) (321)	3.082
		8	3.068	(250) (520)	3.065
2	3.02	20	3.006	(141) (411)	3.005
1/2	2.91	7	2.919	(610)	2.919
4	2.70	4	2.805	(331)	2.804
		25	2.776	(421) (241)	2.775
		3	2.764	(440)	2.763
		2	2.736	(350) (530)	2.734
1/2	2.70	4	2.693	(151)	2.691
		2	2.575	(061) (601)	2.567
		3	2.547	(341)	2.545
1/2	2.54	3	2.539	(710)	2.535
		1	2.499	(251)	2.501
		3	2.453	(540)	2.451
1	2.42	7	2.419	{ (161)	2.420
				{ (360) (630)	2.411
		2	2.328	(441)	2.328
1/2	2.30	6	2.313	{ (071) (701)	2.311
				{ (521)	2.311
1	2.25	9	2.264	(261) (621)	2.262
		3	2.241	(180)	2.240
		6	2.200	(550)	2.210
		6	2.194	{ (460) (640)	2.195
				{ (171) (711)	2.187
1	2.16	13	2.164	(002)	2.163
		13	2.158	(730)	2.153
2	2.13	20	2.135	(451) (541)	2.132
		4	2.108	{ (202) (022)	2.110
				{ (361)	2.108
		8	2.092	{ (801)	2.094
				{ (280)	2.088
2	2.06	14	2.059	(271) (721)	2.057

(1) Zinckenite from Wolfsberg, Harz, Germany (Berry & Thompson, 1962)¹⁸⁾(2) Synthetic $Pb_9Sb_{22}S_{42}$ (zinckenite), Indices were determined by the data as follows: hexagonal, $a=22.10 \text{ \AA}$, $c=4.326 \text{ \AA}$.

Differential thermal curve for synthetic zinckenite is vacuum shown in Fig. 2. Two strong endthermic reactions were occurred in temperature range from 540° to 580°C. Among them, former endthermic peak beginning at 540°C shows a incongruent melting reaction of zinckenite to robinsonite and liquid. Later shows a melting reaction with contineously changing chemical composition of liquid along liquidus, and zinckenite was completely melts at 579°C

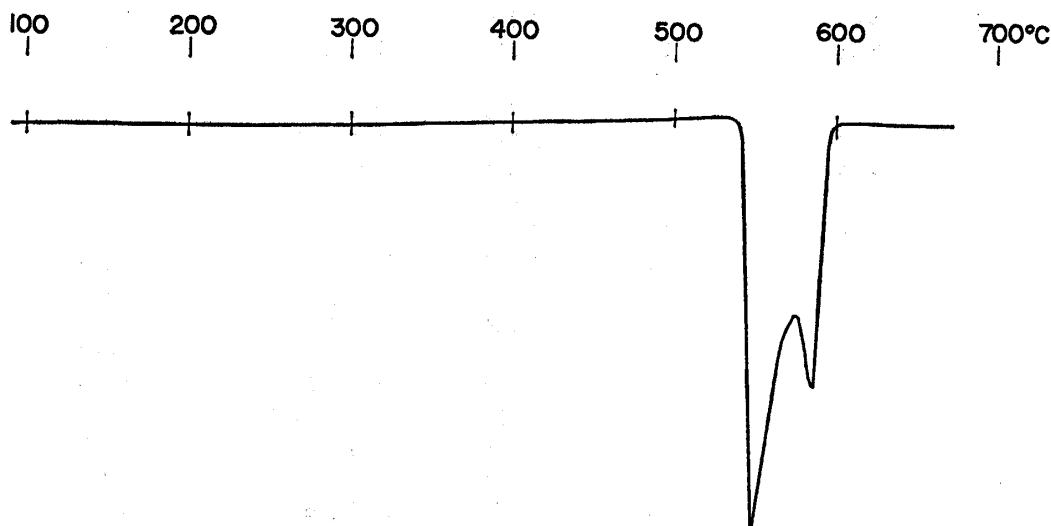


Fig. 2. The differential thermal curve for synthetic $\text{Pb}_9\text{Sb}_{22}\text{S}_{42}$ (zinckenite)

3. $\text{Pb}_4\text{Sb}_6\text{S}_{13}$ (Robinsonite)

Robinsonite, lead-antimony sulfosalt mineral found by Berry et al (1952)¹⁹⁾, was already synthesized by Robinson (1948)^{9,10)}, Berry et al (1952)¹⁹⁾, Kitakaze (1968)^{1,2,3)} and Salanci and Moh(1970)¹²⁾ and others¹³⁾. Synthetic robinsonite is stable below incongruent melting point at 582°C. It was produced by a solid reaction between lead and antimony sulfide. These two sulfide were accurately weighed with molecular ratio of four to three, and were mixed uniformly under acetone in an agate moter. The mixture was sealed in the Hario glass tube under vacuum. The sealed glass tube was put into the electric furnace, and was kept for 5 or 6 days at 530°C. Generally product is mostly homogeneous with aggregate of acicular crystals. After heating, the product was taken out and ground. Then it was again sealed in an evacuated glass tube and heated at 530°C for 6 days. It was cooled slowly in air after heating. Robinsonite from second heating was completely a homogeneous and was aggregate of small needle-like crystals.

Synthetic robinsonite was megascopically lead gray in color with metallic luster. Under the ore microscope, synthetic robinsonite has a weak pleochroism changing its color from white to grayish white with pale bluish tint in air, and strong anisotropism from grayish yellow to dark yellowish brown or dark bluish gray under crossed nicols.

When etched by $\text{HNO}_3(1:1)$, it was quickly tarnished to brown or black, and by fume of $\text{HCl}(1:1)$ and $\text{HgCl}_2(20\%)$ it was slightly stained to brown. By $\text{KOH}(\text{sat.})$, it is tarnished to brown or bluish gray and the reaction is quick in than on boulangerite. However, it is negative for $\text{KCN}(20\%)$ and $\text{FeCl}_3(20\%)$.

The X-ray powder data for synthetic robinsonite are shown in table 2 as compared with natural one¹⁹⁾. The single crystal for robinsonite described by Berry et al (1952)¹⁹⁾ has the unit cell with follow: triclinic, $a=16.51 \text{ \AA}$, $b=17.62 \text{ \AA}$, $c=3.97 \text{ \AA}$, $\alpha=96^\circ 04'$, $\beta=96^\circ 22'$, $\gamma=91^\circ 12'$, space group Pl. The calculated d-value in table 2 was computed by data from Berry et al (1952)¹⁹⁾. Both of the value for d-calc. and d-mess. shows a good accordance. The density for synthetic robinsonite measured by Berman density balance was 5.73 g/cm^3 and calculated density from cell constant was 5.75 g/cm^3 as $Z=2$. Both of them are in very good agreement. The chemical composition for robinsonite was richer than the value of $\text{Pb}_7\text{Sb}_{12}\text{S}_{25}$ by Berry et al¹⁹⁾ on the concentration of lead.

Differential thermal curve for synthetic robinsonite in vacuum is shown in Fig. 3. Three endthermic peaks were observed, among them, the first endthermic peak beginning at 582°C shows a incongruent melting reaction of robinsonite to $\text{Pb}_8\text{Sb}_{10}\text{S}_{23}$ and liquid, and the second endothermic peak beginning at 603°C is thought incongruent melting of $\text{Pb}_4\text{Sb}_6\text{S}_{13}$ to $\text{Pb}_5\text{Sb}_4\text{S}_{11}$ and liquid, and last one shows a liquidus temperature with end point at 630°C .

Table 2. The data of X-ray powder diffraction for synthetic $\text{Pb}_4\text{Sb}_6\text{S}_{13}$.

(1)		(2)		(3)			
I	d	I	d	I	d(meas.)	hkl	d(calc.)
				2	7.675	120	7.620
1/4	7.4	1/4	7.4	10	7.523	2 $\bar{1}$ 0	7.522
				8	7.323	210	7.333
1/2	6.0	1/2	6.1	18	6.090	2 $\bar{2}$ 0	6.086
				2	5.925	220	5.889
				2	5.860	030	5.837
1/2	5.44	1/2	5.44	16	5.465	300	5.466
				6	5.262	3 $\bar{1}$ 0	5.268
		1/2	5.16	1	5.156	310	5.170
				3	4.834	2 $\bar{3}$ 0	4.831
				1	4.720	3 $\bar{2}$ 0	4.707
1/2	4.35	1	4.40	12	4.390	040	4.378
				5	4.270	1 $\bar{4}$ 0	4.265
				5	4.112	400	4.100
8	4.04	7	4.08	70	4.064	3 $\bar{3}$ 0	4.058
8	3.92	7	3.97	70	3.965	410	3.963
						0 $\bar{1}$ 1	3.919
				30	3.904	$\bar{1}$ 01	3.917
						$\bar{1}$ $\bar{1}$ 1	3.907
6	3.79	5	3.80	30	3.817	240	3.810

Table 2. continued

(1)		(2)		(3)			
I	d	I	d	I	d(meas.)	hkl	d(calc.)
				15	3.713	{121	3.717
						{201	3.706
6	3.66	6	3.68	55	3.671	420	3.667
				3	3.630	{211	3.563
						{111	3.560
5	3.47	3	3.49	25	3.507	050	3.502
						{150	3.448
				30	3.450	{121	3.448
						{021	3.443
						{131	3.415
10	3.39	10	3.41	100	3.412	{430	3.408
						{150	3.402
				10	3.375	301	3.374
						{211	3.310
				3	3.310	{131	3.307
						{430	3.304
						{311	3.269
		1/2	3.28	4	3.270	{211	3.264
						{231	3.261
				4	3.252	{250	3.260
						{510	3.243
6	3.18	6	3.19	50	3.206	510	3.205
						{131	3.111
				4	3.109	{520	3.105
						{031	3.103
						{440	3.043
8	3.03	6	3.04	60	3.041	{520	3.039
						{311	3.036
		1	2.96	5	2.976		
				4	2.926		
2	2.88	1	2.89	25	2.904		
2	2.81	1/2	2.82	15	2.835		
				5	2.809		
8	2.75	8	2.74	25	2.767		
				5	2.734		
8	2.67	7	2.68	40	2.686		
1	2.59	3	2.59	25	2.580		
				3	2.546		
		1/2	2.53	3	2.525		
				5	2.422		
2	2.33	3	2.34	15	2.345		
				3	2.309		
2	2.27	1/2	2.26	15	2.279		
				3	2.238		
				3	2.201		
1	2.18	1/2	2.19	5	2.192		
		1	2.13	8	2.135		
				8	2.123		
4	2.11	3	2.09	8	2.107		
				3	2.087		
3	2.05	1	2.04	8	2.059		

3	1.969	1/2	1.973	10	1.984
				6	1.914
6	1.862	2	1.862	10	1.885
				8	1.871
				6	1.857

- (1) Natural robinsonite from Red Bird mine, Nevada.¹⁹⁾
 (2) Artificial crystal by Berry et al. (1952)¹⁹⁾
 (3) Synthetic $\text{Pb}_4\text{Sb}_6\text{S}_{13}$ (robinsonite), indices were calculated by the cell constant as follows: $a=16.51 \text{ \AA}$, $b=17.62 \text{ \AA}$, $c=3.97 \text{ \AA}$, $\alpha=96^\circ 04'$, $\beta=96^\circ 22'$, $\gamma=91^\circ 12'$.

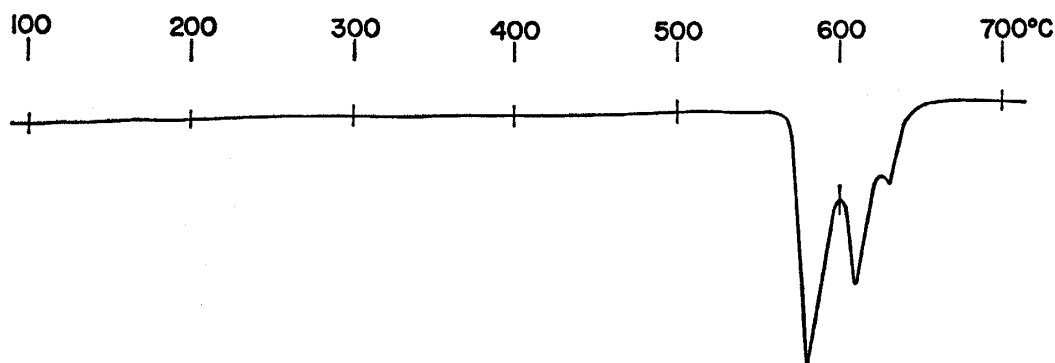


Fig. 3. The curve of the differential thermal analysis for synthetic $\text{Pb}_4\text{Sb}_6\text{S}_{13}$ (robinsonite)

4. $\text{Pb}_5\text{Sb}_4\text{S}_{11}$ (Boulangerite)

Boulangerite was known as lead-antimony sulfide mineral and was already produced artificially by many workers. Synthetic boulangerite is stable below the incongruent melting temperature at 640°C . This mineral was synthesized by a reaction between lead and antimony sulfides in solid state, these two sulfides were accurately weighed with molecular ratio on five to two, and were mixed under acetone. The mixture was sealed in the silica glass tube and heated at 600°C for 6 days. After heating, product was taken out and ground, and was heated at 600°C for 6 days in the evacuated silica glass tube. A homogenous product obtained by the second heating is aggregate of acicular crystals with 0.1 to 1 mm in size and megascopically lead gray in color with metallic luster.

Under the ore microscope, synthetic boulangerite has a weak pleochroism changing its color from grayish white to white with bluish green tint in air, and shows strong anisotropism with its interference color from light yellow to brown or bluish gray under crossed nicols.

When etched by $\text{HNO}_3(1:1)$, it slowly stain to brown or black. By fume of $\text{HCl}(1:1)$, it is tarnished and by $\text{KOH}(\text{sat.})$ and $\text{HgCl}_2(20\%)$ is tarnished to brown. But it is the negative for $\text{KCN}(20\%)$ and $\text{FeCl}_3(20\%)$.

The X-ray powder diffraction data for synthetic boulangerite are given in Table 3 compared with natural boulangerite. The single crystal data for synthetic boulangerite were measured on oscillation and Weissenberg photographs

Table 3. The X-ray powder data for synthetic $Pb_5Sb_4S_{11}$.

(1)		(2)		(3)			
I	d(meas.)	I	d(meas.)	I	d(meas.)	(hkl)	d(calc.)
		6	6.81	7	6.763	(310)	6.770
		12	6.09	10	6.061	(320)	6.057
		3	5.19	2	5.173	(410)	5.172
		3	4.85	3	4.829	(420)	4.832
		6	4.61	3	4.585	(150)	4.585
		12	4.41	9	4.387	(430)	4.390
				2	4.175	(510)	4.174
		12	3.99	8	3.982	(520)	3.990
				15	3.929	(440)	3.935
2	3.93	30	3.93	25	3.910	{(060)	3.913
						{(350)	3.912
						{(111)	3.892
		18	3.86	15	3.847	(160)	3.848
10	3.72	100	3.74	100	3.731	{(121)	3.741
						{(530)	3.729
						{(211)	3.709
		30	3.68	22	3.675	(260)	3.671
		4	3.54	4	3.531	(600)	3.535
				2	3.493	(301)	3.493
1	3.44	17	3.45	19	3.438	(540)	3.438
2	3.30	22	3.32	23	3.313	(170)	3.313
4	3.21	45	3.23	45	3.220	(630)	3.222
				8	3.191	{(270)	3.198
						{(331)	3.189
4	3.01	40	3.03	35	3.030	{(640)	3.028
						{(151)	3.021
				15	3.009	{(710)	3.005
						{(341)	3.002
				18	2.968	(431)	2.964
						{(080)	2.935
				5	2.940	{(251)	2.933
						{(720)	2.934
9	2.81	50	2.826	45	2.826	{(280)	2.829
						{(730)	2.826
		25	2.792	20	2.810	{(441)	2.811
						{(061)	2.803
				20	2.782	(161)	2.779
		6	2.723	5	2.712	{(380)	2.711
						{(261)	2.710
3	2.68	25	2.698	25	2.695	(740)	2.692
		6	2.652	2	2.654	(800)	2.651
				3	2.645	(451)	2.645
1/2	2.59	18	2.592	9	2.587	(820)	2.586
				2	2.542	(290)	2.535
1/2	2.51	6	2.515	3	2.512	(830)	2.511
		3	2.456	1	2.444	(390)	2.448
		9	2.429	5	2.420	(371)	2.419
		15	2.373	10	2.370	(721)	2.369
2	2.33	18	2.346	12	2.342	{(0, 10, 0)	2.348
						{(910)	2.345
						{(490)	2.341

Table 3. continued

(1)		(2)		(3)			
I	d(meas.)	I	d(meas.)	I	d(meas.)	(hkl)	d(calc.)
3	2.14	12	2.318	6	2.313	(471)	2.316
						(281)	2.313
						(920)	2.311
						(850)	2.309
						(381)	2.247
						(590)	2.222
						(3, 10, 0)	2.228
						(821)	2.174
						(751)	2.150
						(4, 10, 0)	2.147
							2.148
							2.130
							2.121
							2.098
							2.055
	2.008						
	1.990						
	1.968						
	1.947						
	1.931						
	1.922						
	1.862						

(1) Natural boulangerite from Babine bonanza, Omineca, B.C.²⁰⁾

(2) Natural boulangerite from Obira mine, Kyushu, Japan

(3) Synthetic $Pb_5Sb_4S_{11}$, cell constant is follows: orthorhombic, $a=21.21 \text{ \AA}$, $b=23.48 \text{ \AA}$, $c=4.02 \text{ \AA}$.

has the cell constant with following: orthorhombic, $a=21.38 \text{ \AA}$, $b=23.43 \text{ \AA}$, $c=4.02 \text{ \AA}$, space group Pbnm. Natural boulangerite with following cell constant: $a=21.56 \text{ \AA}$, $b=23.51 \text{ \AA}$, $c=8.09 \text{ \AA}$, $\beta=100^\circ 48' 20''$, has a super lattice for synthetic boulangerite, and synthetic mineral has about half of the natural one in c value. The calculated d-value in Table 3 was computed by single crystal data, and both of these values show very good agreement. The density for aggregate of needle crystals of boulangerite measured by Berman density balance was 6.24 g/cm^3 and calculated from cell constant as $Z=4$ was 6.23 g/cm^3 , and these two values are in good agreement.

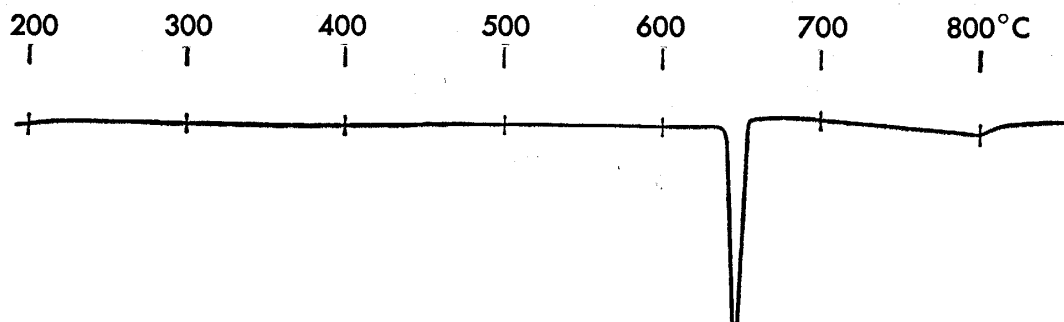


Fig. 4. The curve of differential thermal analysis for synthetic $Pb_5Sb_4S_{11}$ (boulangerite)

The differential thermal curve of synthetic boulangerite in evacuated silica glass tube is given in Fig. 4. A strong endothermic peak beginning at 640°C and a widespread small endothermic peak ending at 800°C were observed. A former peak is thought two reactions overlapped. They are incongruent melting of boulangerite to $\text{Pb}_3\text{Sb}_2\text{S}_6$ and liquid, and of $\text{Pb}_3\text{Sb}_2\text{S}_6$ to PbS and liquid. Later endothermic peak shows a reaction with continuously changing its chemical composition of liquid.

5. $\text{Pb}_2\text{Sb}_2\text{S}_5$ (New phase)

During the study on the phase relation in the PbS-Sb₂S₃ system^{1)2,3)}, new synthetic $\text{Pb}_2\text{Sb}_2\text{S}_5$ was found as one of the stable phase. The new phase is stable at temperature below 600°C. Although lower stability limit of the new phase was not made clear, at 400°C, it is stable with chemical composition of slightly sulfur richer²¹⁾ than $\text{Pb}_2\text{Sb}_2\text{S}_5$ and assembled with boulangerite and robinsonite.

The synthesis of $\text{Pb}_2\text{Sb}_2\text{S}_5$ phase was performed by a reaction between lead and antimony sulfides. Two sulfides were weighed accurately with molecular ratio of two to one, and mixed thoroughly under acetone. The mixture sealed in a evacuated Hario glass tube were heated at 550°C for 6 days in an electric furnace. After heating product was taken out and ground under acetone to be mixed uniformly. It was again sealed in a evacuated glass tube and reheated at 550°C for 12 days. Synthetic product is homogeneous and is fully sintered aggregate of $\text{Pb}_2\text{Sb}_2\text{S}_5$. The new phase is megacrystically lead gray with metallic luster.

Under the ore microscope, synthetic $\text{Pb}_2\text{Sb}_2\text{S}_5$ has a weak pleochroism changing in color from white to grayish white, and strong anisotropism from grayish yellow to dark brown or dark yellowish brown in its interference color. When etched by $\text{HNO}_3(1:1)$, it is slightly stained to brown or black. By $\text{KOH}(\text{sat.})$ and $\text{HgCl}_2(20\%)$, it is slightly tarnished to brown or bluish gray. However, it is negative to $\text{FeCl}_3(20\%)$ and $\text{KCN}(20\%)$.

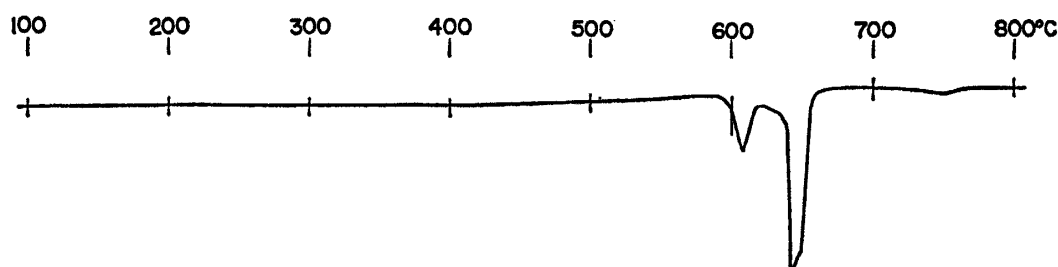
The data of X-ray powder diffraction for synthetic $\text{Pb}_2\text{Sb}_2\text{S}_5$ is shown in Table 4. The single crystal data for the new phase was measured on the oscillation and Weissenberg photographs and the following unit cell values were obtained: monoclinic, $a=50.2 \text{ \AA}$, $b=4.03 \text{ \AA}$, $c=20.15 \text{ \AA}$, $\beta=114^\circ 50'$, space group C2/m. The calculated d-values were obtained by calculation used to the cell constant for the new phase and compared with measured d-values in table 4. Both of two values are in good agreement. The density of sintered aggregate for $\text{Pb}_2\text{Sb}_2\text{S}_5$ was measured by Berman density balance, and was 6.09 g/cm^3 . The calculated density from cell constant as $Z=17$ was 6.07 g/cm^3 . Both values are in good accordance.

The differential thermal curve for $\text{Pb}_2\text{Sb}_2\text{S}_5$ given in Fig. 4 shows three endothermic peaks in temperature range from 600° to 750°C. Among them,

Table 4. The X-ray powder data for synthetic $\text{Pb}_2\text{Sb}_2\text{S}_5$.

I	d(meas.)	hkl	d(calc.)*	I	d(meas.)	hkl	d(calc.)*
3	9.37	002	9.43	5	3.260	14, 0, 0	3.260
1	8.31	401	8.34	9	3.062	804	3.058
8	7.63	{202	7.66	13	3.006	91 $\bar{4}$	3.003
		{600	7.61	30	2.964	{513	2.968
3	6.83	{40 $\bar{3}$	6.86			{80 $\bar{7}$	2.964
		{20 $\bar{3}$	6.84	20	2.928	605	2.926
3	6.23	003	6.29	2	2.867	{71 $\bar{5}$	2.872
9	6.13	402	6.12			{11, 1, $\bar{4}$	2.867
1	5.51	203	5.50	2	2.855	16, 0, 0	2.852
1	5.20	40 $\bar{4}$	5.20	7	2.803	91 $\bar{5}$	2.808
2	4.56	10, 0, 0	4.56	18	2.784	{13, 1, $\bar{2}$	2.790
5	4.29	10, 0, $\bar{4}$	4.31			{912	2.782
13	4.16	802	4.17	14	2.775	13, 1, $\bar{3}$	2.775
15	4.13	40 $\bar{5}$	4.14	9	2.747	13, 1, $\bar{1}$	2.744
		{603	4.08	20	2.677	805	2.673
45	4.08	{12, 0, $\bar{1}$	4.08	20	2.597	80 $\bar{8}$	2.598
		{10, 0, 1	4.06	10	2.582	10, 0, $\bar{8}$	2.584
8	4.02	80 $\bar{5}$	4.02	4	2.567	{18, 0, $\bar{6}$	2.571
8	3.834	404	3.827			{913	2.564
6	3.806	12, 0, 0	3.804	3	2.530	18, 0, 0	2.536
10	3.789	10, 0, $\bar{5}$	3.794	2	2.508		
		{31 $\bar{2}$	3.729	4	2.431		
13	3.727	{11 $\bar{2}$	3.727	2	2.377		
		{311	3.721	5	2.373		
40	3.576	{14, 0, $\bar{2}$	3.581	5	2.329		
		{14, 0, $\bar{3}$	3.572	6	2.308		
70	3.467	{14, 0, $\bar{1}$	3.466	15	2.287		
		{60 $\bar{6}$	3.464	13	2.270		
100	3.423	51 $\bar{3}$	3.434	3	2.253		
		11 $\bar{3}$	3.430	7	2.239		
		80 $\bar{6}$	3.428				
		604	3.416				

* Indices were determined by the single crystal data as follows: monoclinic, $a=50.2 \text{ \AA}$, $b=4.03 \text{ \AA}$, $c=20.15 \text{ \AA}$, $\beta=114^\circ 50'$.

Fig. 5. The differential thermal curve for synthetic $\text{Pb}_2\text{Sb}_2\text{S}_5$.

the first peak is thought a decomposition of $\text{Pb}_2\text{Sb}_2\text{S}_5$ at 600°C or incongruent melting reaction of $\text{Pb}_2\text{Sb}_2\text{S}_5$ to $\text{Pb}_5\text{Sb}_4\text{S}_{11}$ and liquid. The second one shows two endthermic reactions which are incongruent melt of $\text{Pb}_5\text{Sb}_4\text{S}_{11}$ to $\text{Pb}_3\text{Sb}_2\text{S}_6$ and liquid, and of $\text{Pb}_3\text{Sb}_2\text{S}_6$ to PbS and liquid in narrow temperature range from

640°C to 650°C. Last widespread small endthermic peak with end point at 750°C shows a melting reaction with changing its chemical composition of liquid coexisting PbS.

Reference

- 1) A. Kitakaze: Unpub. M. S. thesis, Yamaguchi Univ., in Japanese (1968)
- 2) A. Kitakaze and H. Shima: Jap. Assoc. Pet. Min. Econ. Geol., **59**, 167-168 (1968) Abs. in Japanese
- 3) A. Sugaki, H. Shima and A. Kitakaze: Ditto, **61**, 172-173 (1969) Abs. in Japanese
- 4) A. Sugaki and H. Shima: Mem. Fac. Eng. Yamaguchi Univ., **15**, 15-31 (1965)
- 5) ———, ———: Ditto, **15**, 33-47 (1965)
- 6) ———, ———: Ditto, **16**, 109-118 (1965)
- 7) ———, ——— and A. Kitakaze: Tech. Report. Yamaguchi Univ., **1**, 71-85 (1972)
- 8) D. Iitsuka: Kyoto Emp. Univ. Coll. Sci. Mem., **4**, 61-64 (1920)
- 9) S. C. Robinson: Econ. Geol., **43**, 293-312 (1948)
- 10) ———: Univ. Toronto Studies, Geol. Ser., No. 52, 54-70 (1948)
- 11) J. L. Jambor: Can. Min., **9**, 505-521 (1968)
- 12) B. Salanci and G. H. Moh: N. Jb. Min. Mh., **11**, 524-258 (1970)
- 13) J. R. Craig and P. B. Barton, Jr.: Econ. Geol., **68**, 493-506 (1973)
- 14) M. N. Short: Microscopic Determination of the ore Minerals, U. S. G. S. Wash. Bul. 914 (1940) p.
- 15) P. Ramdohr: The ore Minerals and their Intergrowths, Pergamon P press N. Y. (1969)
- 16) W. Uytendogaadt: Table for Microscopic Identification of ore Minerals, Princeton Univ. Press, Princetone (1951)
- 17) R. Sadanaga and H. Takeda: Min. Jour., **4**, 159-171 (1964)
- 18) L. G. Berry, and R. M. Thompson: X-ry Powder Data for Ore Minerals, 85, Geol. Soc. Am., N.Y. (1962). No. 207
- 19) ———, J. J. Fahry and E. H. Bailey: Amer. Min., **37**, 439-446 (1952)
- 20) ——— and R. M. Thompson: X-ray Powder Data for Ore Minerals, 85, Geol. Soc. Am., N.Y. (1962), No. 171
- 21) T. Yamamoto, A. Sugaki, H. Shima and A. Kitakaze: Jap. Assoc. Pet. Min. Econ. Geol., **68**, 94 (1973) Abs. in Japanese